Journal of Applied Polymer Science

Synthesis, thermal and mechanical behavior of a silicon/phosphorus containing epoxy resin

Cong Peng,[1] Zhanjun Wu,[1] Jialiang Li,[1] Zhi Wang,[1] Hongyu Wang,[1] Ming Zhao[2]

[1]School of Aeronautics and Astronautics, Faculty of Vehicle Engineering and Mechanics, State Key Laboratory of Structural Analysis for Industrial Equipment, Dalian University of Technology, Dalian 116024, People's Republic of China

[2]Department of Engineering Mechanics, Faculty of Vehicle Engineering and Mechanics, State Key Laboratory of Structural Analysis for Industrial Equipment, Dalian University of Technology, Dalian 116024, People's Republic of China

Correspondence to: Z. Wang (E-mail: wzdlut@dlut.edu.cn)

ABSTRACT: A liquid silicon/phosphorus containing flame retardant (DOPO–TVS) was synthesized with 9,10-dihydro-9-oxa-10-phosphapheanthrene-10-oxid (DOPO) and triethoxyvinylsilane (TVS). Meanwhile, a modified epoxy resin (IPTS–EP) was prepared by grafting isocyanate propyl triethoxysilane (IPTS) to the side chain of bisphenol A epoxy resin (EP) through radical polymerization. Finally, the flame retardant (DOPO–TVS) was incorporated into the modified epoxy resin (IPTS–EP) through sol–gel reaction between the ethyoxyl of the two intermediates to obtain the silicon/phosphorus containing epoxy resin. The molecular structures of DOPO–TVS, IPTS–EP and the final modified epoxy resin were confirmed by FTIR spectra and ^{1}H-NMR, ^{31}P-NMR. Thermogravimetric analysis (TGA), differential scanning calorimetry, and limiting oxygen index were conducted to explore the thermal properties and flame retardancy of the synthesized epoxy resin. The thermal behavior and flame retardancy were improved. After heating to 600°C in a tube furnace, the char residue of the modified resin containing 10 wt % DOPO–TVS displayed more stable feature compared to that of pure EP, which was observed both by visual inspection and scanning electron microscope (SEM). Moreover, the mechanical performance testing results exhibited the modified epoxy resins possessed elevated tensile properties and fracture toughness which is supported by SEM observation of the tensile fracture section. © 2015 Wiley Periodicals, Inc. J. Appl. Polym. Sci. **2015**, *132*, 42788.

KEYWORDS: flame retardance; mechanical properties; thermal properties

Received 16 June 2015; accepted 28 July 2015

DOI: 10.1002/app.42788

INTRODUCTION

Epoxy resins (EPs) have been widely used as matrix resin for structural compositions and electronic parts due to its merits of easy handling and processability, low shrinkage after curing, superior electrical and mechanical properties, and remarkable adhesion to many substrates.[1–3] However, poor flammability and thermal stability limits its use in those areas which demand high heat resistance and good flame retardant behavior. Many methods have been developed to improve its thermal stability and flame retardancy.[4–7]

Phosphorus has many advantages as a flame retardant element added to the polymer matrix. Its high flame retardant efficiency, low flue gas release, and small hazard to ecological environment during combustion makes it the most promising substitute of halogen containing flame retardant.[8] 9,10-Dihydro-9-oxa-10-phosphapheanthrene-10-oxid (DOPO) is a kind of widely used phosphorus-containing flame retardant with high reactivity and good flame retardant performance with EP.[7,9] Tremendous achievements on enhancing the flame retardancy have been reached by incorporating DOPO and its derivatives into EP. DOPO and their derivatives are solid under normal circumstances, which leads to its poor compatibility and dispersibility with the matrix and thus reduces many other performance especially mechanical behavior of the polymer matrix.[10] How to conquer these disadvantages without sacrificing the outstanding flame retardancy of the DOPO series is still a challenging issue.

The Si—O (110 kcal/mol) bond has higher dissociation energy compared to C—C (82.6 kcal/mol) bond and C—O (85.5 kcal/mol) bond. Thus it is capable of forming a network structure which has a high thermal stability.[11,12] Meanwhile, the high thermal stability of Si—O bond could play a role in improving oxidation resistance of the polymer during combustion. During thermal degradation of the polymer materials, silicon element interacts with the polymer matrix, migrates to the surface of the matrix due to its low surface energy, and finally forms a silicon-rich surface layer of solid carbon. Several researches showed

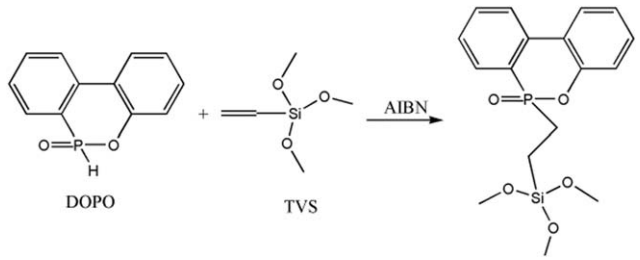

Scheme 1. Synthesis of the phosphorous–silicon containing flame retardant (DOPO–TVS).

that the thermal stability of the polymer matrix significantly increased after incorporation of a small amount of silicon-containing compound.[13–15] Moreover, enhancement of flame retardancy of EPs has been achieved by incorporation of phosphorus and silicon into EPs with bringing a P—Si synergistic effect of flame retardancy.[10,11,13–15] While under flame exposure, phosphorus provides a tendency for char formation, silicon provides an enhancement for the thermal stability of the char. Thus introducing both elements may combine these two factors which lead to strong flame retardancy and thermal stability. Besides, Si—O bond is a type of polymer chain which gives flexibility due to their high bond energy and the low rotation barrier energy. Thus, introducing this flexible linkage or chains can effectively improve the toughness of the matrix. However, few studies have been reported on thermal stability and flame retardancy along with the mechanical behaviors for the silicon/phosphorus containing EP.

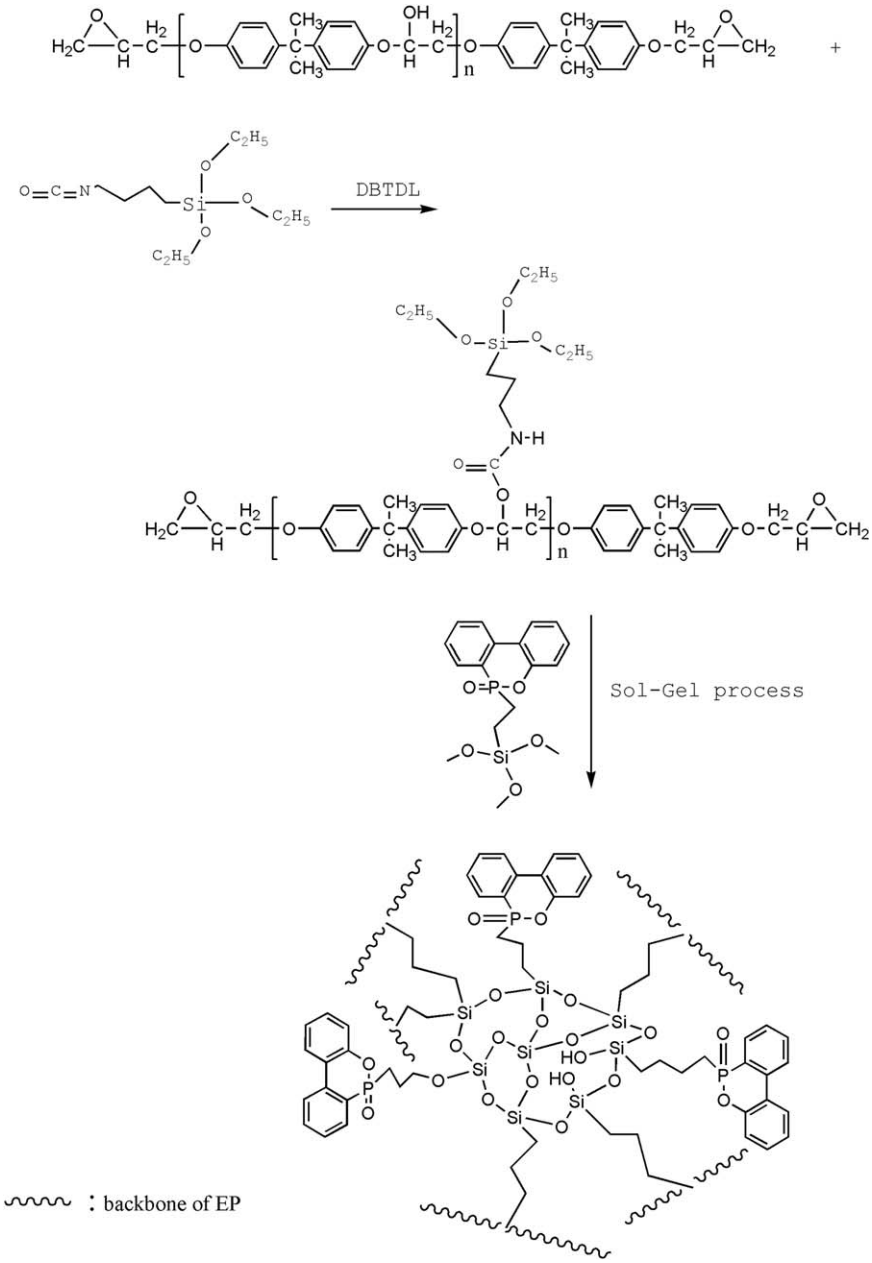

Scheme 2. Synthesis of the phosphorous–silicon containing EP.

Table I. Compositions of the Samples

Sample	E51 content (%)	IPTS content (%)	DOPO-TVS content (%)	Si content (wt %)	P content (wt %)
Pure EP	100	0	0	0	0
EP5	79.2	15.8	5	2.0	0.32
EP10	75	15	10	2.3	0.65
EP15	70.8	14.2	15	2.5	0.98
EP20	66.7	13.3	20	2.7	1.30

In this article, a silicon–phosphorus containing flame retardant was synthesized through the reaction between DOPO and triethoxyvinylsilane (TVS) to improve the thermal stability and flame retardancy of the EP without reducing its mechanical behavior. To create a basis to graft the new flame retardant with EP without consuming the epoxy group, isocyanate propyl triethoxysilane (IPTS) was first grafted onto the side chain of EP through the reaction with hydroxyl of the EP. In the last step, the new flame retardant DOPO–TVS was grafted to the side chain of EP through the mild sol–gel reaction. Thermal stability, flame retardancy, and basic mechanical behaviors of modified EP containing different amount of DOPO–TVS were investigated.

EXPERIMENTAL

Materials

Diglycidyl ether of bisphenol A (epoxy equivalent 0.51 mol/100 g, EP) was purchased from FeiCheng DeYuan Chemicals. 2,2′-azobisisobutyronitrile (AIBN) and 4,4′-diaminodiphenylmethane (DDM) were purchased from TianJin GuangFu Fine Chemical Research Institute. DOPO, industrial grade (purity 97.0%), was purchased from Huizhou Sunstar Technology, China. TVS was obtained from AB Specialty Silicones. IPTS was from Energy Chemical. Dibutyltindilaurate (DBTDL) was purchased from Adamas Reagent. All other materials are analytically pure and used without any treatment.

Preparation of Silicon–Phosphorus Containing Flame Retardant DOPO–TVS

DOPO (21.6 g/0.1 mol) and methylbenzene (30 mL) was blended in a three-neck flask equipped with stirring bar, reflux condenser, constant pressure dropping funnel in N_2 atmosphere. Then the mixture was heated to 80°C. AIBN (0.1 g) and TVS (14.8 g/0.1 mol) in 20 mL methylbenzene was added dropwise to the flask in about 2 h. The temperature remained at 80°C for 24 h. At last, light yellow transparent viscous liquid was obtained after methylbenzene was distilled off under reduced pressure. The schematic diagram of DOPO–TVS is demonstrated in Scheme 1.

Preparation of Modified Epoxy Resin IPTS–EP

120 g diglycidyl ether of biphenol A (symbolized EP in the following text), 24 g IPTS, 0.1 g DBTDL was blended in a 250 mL three-neck flask equipped with stirring bar in N_2 atmosphere. Then the mixture was heated to 50°C. The temperature was maintained until the characteristic infrared absorption peak of isocyanato at 2275 cm^{-1} disappeared and colorless viscous modified EP was obtained (symbolized IPTS–EP).[16] This process is shown on the top of Scheme 2.

Preparation of the Final Product: Silicon–Phosphorus Containing EP

IPTS–EP and DOPO–TVS were blended in different ratio (typically, EP5 indicates that the mass fraction of DOPO–TVS in the modified EP is 5% etc.). Acetone and ethyl alcohol were used as solvent. Distilled water was added to initiate sol–gel process. The molar ratio of water to ethoxy was 1.5 : 1.[17] Acetic acid was added as the catalyst[18] of the hydrolysis reaction to acquire a pH 3–4 environment. The mixture was heated to 50°C and remained for 5 h. At last, water and solvent was distilled off under reduced pressure to obtain light yellow transparent viscous silicon–phosphorus containing EP. This process is showed in Scheme 2. Detailed content of each ingredient is listed in Table I.

Curing Procedure of the Silicon–Phosphorus Containing EP

DDM and the final product were blended at the molar ratio of one amino hydrogen to one epoxy group. The mixture was vigorously stirred at 80°C until DDM completely dissolved. The liquid mixture was poured into mold after vacuum degassing and cured in an oven under the process of 100°C (2 h)−130°C (2 h)−160°C (4 h). Finally, the mold was gradually cooled to room temperature, and silicon–phosphorus containing EP hybrid was obtained.

Characterization

FTIR spectra were measured with a Perkin Elmer Spectrum One FTIR from 4000 cm^{-1} to 600 cm^{-1} (KBr). ^{1}H-NMR,^{31}P-NMR were measured on Varian INOVA at the frequency of 500 MHz

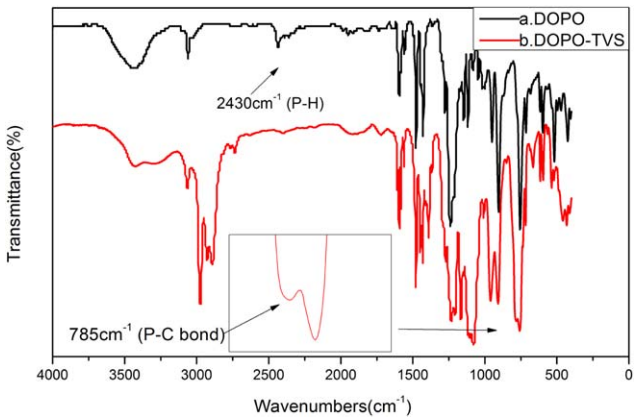

Figure 1. FTIR of DOPO and DOPO–TVS. [Color figure can be viewed in the online issue, which is available at wileyonlinelibrary.com.]

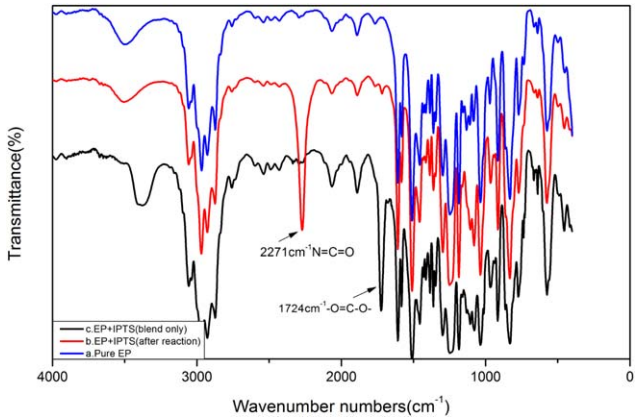

Figure 2. FTIR of pure EP and EP+IPTS (only blended and after reaction). [Color figure can be viewed in the online issue, which is available at wileyonlinelibrary.com.]

and 202 MHz, respectively, in $CDCl_3$. Differential scanning calorimetric (DSC) thermograms were recorded with a thermal analysis DSC-Q10 in N_2 flow of 40 mL/min with heating rate of 10°C/min from 25°C to 250°C. Thermal gravimetric analysis (TGA) was carried out with a TA TGA Q500 at heating rate of 20°C/min from 35°C to 600°C under N_2 atmosphere (100 mL/min). The micromorphology images of the residues after TGA test were obtained using a QUANTA 450 tungsten filament scanning electron microscope (SEM) at high vacuum conditions with a voltage of 20 kV. The limiting oxygen index (LOI) values were performed on an FTT (Fire Testing Technology, UK) Dynisco LOI instrument according to ASTM D2863-97 with sheet dimensions 130 mm × 6.5 mm × 3.2 mm. Tensile strength and fracture toughness was measured on an SDS-100 electro-hydraulic servo testing machine following ASTM D638-99 and ASTM D5045-14, respectively.

RESULTS AND DISCUSSION

Characterization of DOPO–TVS, IPTS–EP, and Silicon–Phosphorus Containing EP

The structure of the product was characterized by FTIR, ^{1}H-NMR, ^{31}P-NMR. The FTIR of DOPO and DOPO–TVS is shown in Figure 1. The most important absorption peak we concern about is the P—H peak near 2358 cm^{-1}.[19,20] Compared to Figure 1(a), the absorption peak in Figure 1(b) almost disappeared which proves that the P—H structure in DOPO is almost consumed by the reaction between DOPO and TVS. Moreover, we can notice in Figure 1(b) that the absorption peak in 785 cm^{-1} is broader compared that of DOPO in Figure 1(a). This is because the generated P—C bond overlaps the original one in this area. Figure 2 shows the FTIR of pure EP, the mixture of EP and IPTS (before reaction), and IPTS–EP (after reaction).The peak of C═N═O at 2271 cm^{-1} almost disappears in Figure 2(b). A new strong peak of O—C═O at 1724 cm^{-1} appeared in Figure 2(c). These confirm that IPTS was successfully grafted onto the backbone of EP. Figure 3(a,b) are the regional FTIR of pure EP and EP–IPTS+10% DOPO–TVS after sol–gel process at 1000 cm^{-1} to 1200 cm^{-1}. The absorption peak of Si—O—Si asymmetric stretching is within the range of 1050 cm^{-1} to 1130 cm^{-1} depending on density of silica according to relevant research.[21] FTIR spectra of the sol–gel final product indicate a distinct absorption peak at 1087 cm^{-1} with a shoulder around 1110 cm^{-1} which confirms the existence of silica network by sol–gel reaction.

Figure 4(a–c) are the ^{1}HNMR of DOPO, TVS, and DOPO–TVS, respectively. Peak 'a' (δ8.64–8.65) is the peak of atom hydrogen in P—H bond.[19] In Figure 4(c), the strength of peak 'a' significantly decreases (peak 'b' corresponds to atom H in benzene ring which does not change in the reaction. Take the strength of peak 'b' as reference. In Figure 4(a), the ratio of strength of 'a/b' is 1/17. While that in Figure 4(c) is 1/374, which is 1/12 of the original value). Peak 'd' (δ5.99–6.02) corresponds to atom hydrogen of double bond in TVS. We can also see an obvious decline of the peak 'd' in Figure 4(c) (peak 'c' corresponds to atom hydrogen in methylene of ethoxy of TVS which does not change in the reaction. Take the strength of peak 'c' as reference. In Figure 4(b), the ratio of strength of 'd/c' is about 1/2 while that in Figure 4(c) is about 1/23, which is about 1/11 of the original value).The consumption of P—H and C═C are reasonably coincident which indicates that the reaction was carried on as expected. The incomplete reaction may be due to the space steric effect in the last phase of the reaction.

^{1}H NMR (500 MHz, Chloroform-*d*) a. δ 8.65 (s, 1H), b. δ8.11–7.13 (m, 17H). [Figure 4(a)].

^{1}H NMR (500 MHz, Chloroform-*d*) d. δ 6.18–5.80 (m, 1H), c. δ3.82 (dd, J = 6.9, 0.8 Hz, 2H), e. δ1.20 (td, J = 6.9, 0.8 Hz, 3H) [Figure 4(b)].

^{1}H NMR (500 MHz, Chloroform-*d*) a. δ 8.63 (s, 1H), b. δ8.02–7.09 (m, 374H), d. δ6.31–5.78 (m, 11H), c. δ3.75 (dd, J = 6.9, 0.7 Hz, 250H), e. δ1.37–0.72 (m, 465H) [Figure 4(c)].

Figure 5(a,b) show the ^{31}P-NMR of DOPO and DOPO–TVS, respectively. Peak 'A' which corresponds to atom phosphorus in DOPO reduces significantly and a new strong peak 'B' appears near 39.5 ppm which corresponds to atom phosphorus in DOPO–TVS.

^{31}P-NMR (202 MHz, Chloroform-*d*) δ 14.65 [Figure 5(a)].

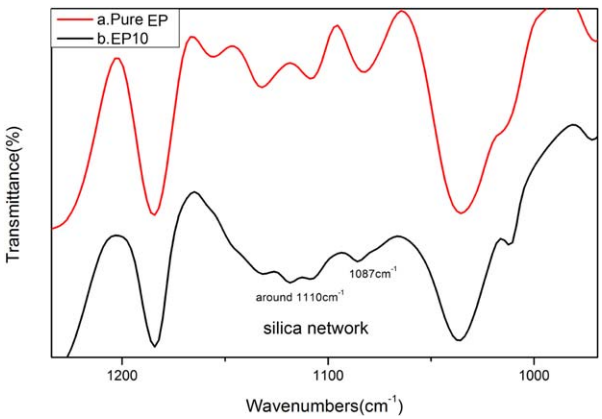

Figure 3. FTIR of pure EP and EP–IPTS+DOPO–TVS after sol–gel process. [Color figure can be viewed in the online issue, which is available at wileyonlinelibrary.com.]

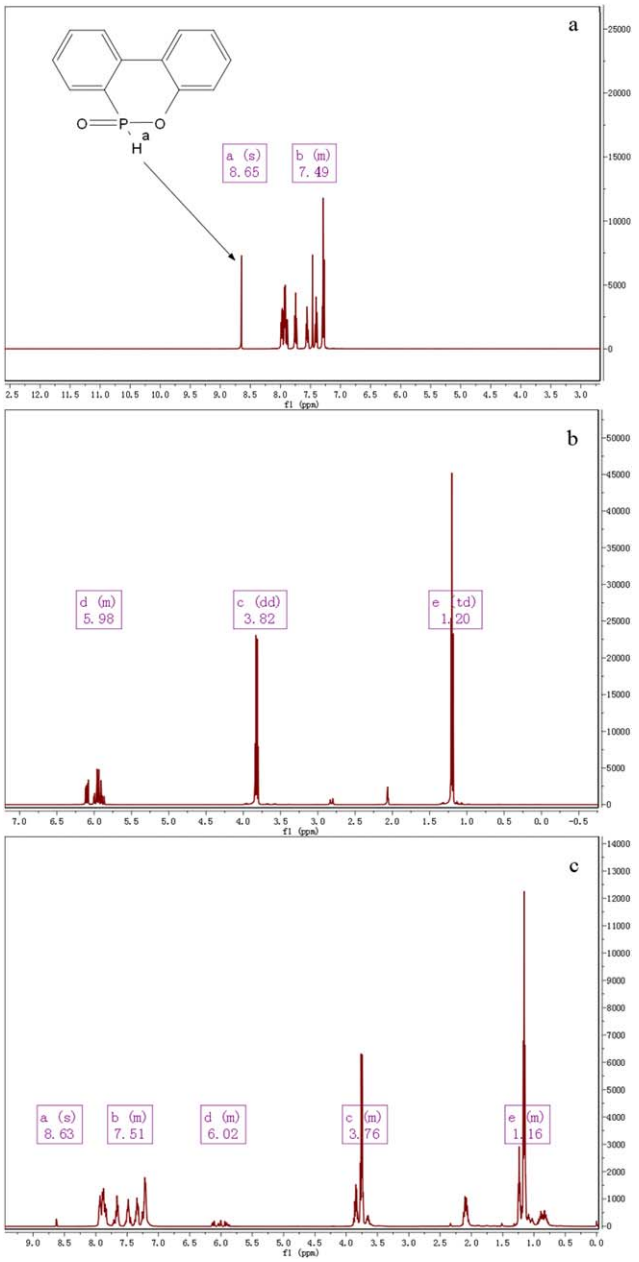

Figure 4. [1]H-NMR of DOPO (a) TVS (b), and DOPO–TVS (c). [Color figure can be viewed in the online issue, which is available at wileyonlinelibrary.com.]

[31]P-NMR (202 MHz, Chloroform-*d*) δ 39.50, 14.51 [Figure 5(b)].

Since the self-condensation of DOPO–TVS, some silica group cannot be grafted onto the EP. To investigate the grafting efficiency, the silica monomers which is not grafted was separated through centrifugation. The precipitation was washed with acetone and centrifuged again. The remained acetone was removed in an oven at 70°C for 1 h. Even for EP20, the silica monomer separated through centrifugation is very slight (4 g IPTS–EP, 1 g DOPO–TVS, the separated silica monomer is just 0.014 g). It indicates that most of the DOPO–TVS are grafted on the EP.

Thermal Properties and Flame Retardancy

The TG and DTG curves of EP and the EP/DOPO–TVS hybrid material measured at heating rate of 10°C/min from room temperature to 600°C are shown in Figure 6(a,b), respectively. The weight-loss curves for the pure EP and modified epoxy hybrids imply a one-step degradation mechanism. Obviously, it can be seen in Figure 6(a) that char residues of the modified EP/DOPO–TVS hybrids are all higher than that of the pure EP. The char yield of pure EP at 600°C is 21.7% while that of the modified EP/DOPO–TVS with 10% DOPO–TVS is as high as 31.7% which is 46% higher than that of the pure EP. However, it must be noted that the increases of the residue weight and the content of DOPO–TVS are not synchronized. The hybrid with 10% content of DOPO–TVS exhibited the highest residue weight. It can be explained as follows: not all DOPO–TVS monomers are grafted onto the network structure. Self-polymerization inevitably occurs during sol–gel process between DOPO–TVS monomers. The more DOPO–TVS, the larger the molecular weight of the self-polymerization product, and the harder for its being grafted onto the EP backbone. These free self-polymerization products have weaker interaction with the matrix and are easier to decompose. The thermal stability of hybrids was lower than pure EP at the first stage of

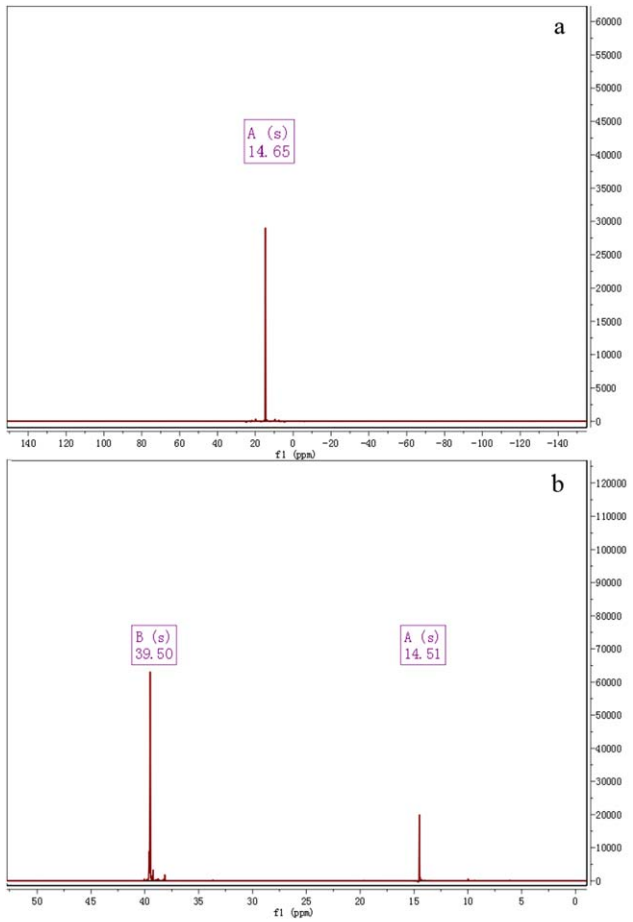

Figure 5. [31]P-NMR of DOPO (a) and DOPO–TVS (b). [Color figure can be viewed in the online issue, which is available at wileyonlinelibrary.com.]

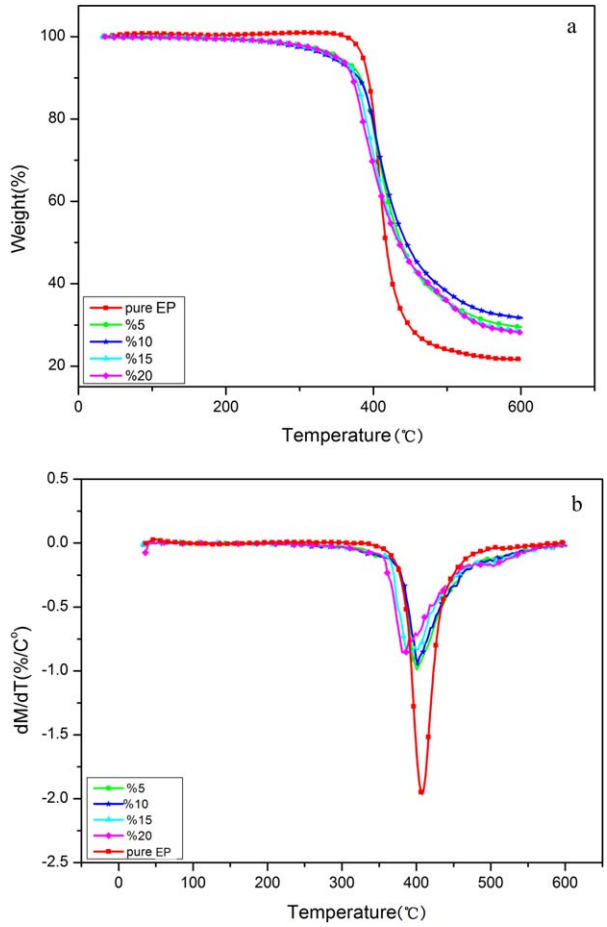

Figure 6. TG (a) and DTG (b) curves in N_2. [Color figure can be viewed in the online issue, which is available at wileyonlinelibrary.com.]

decomposition owing to the weak bonding strength of phosphorus bonds.[22] They form a surface layer of protective char during combustion before the unburned structure materials begin to decompose.[23] As a result, the thermal stability of the hybrids especially for that with 10% DOPO–TVS is much higher than that of pure EP at the high temperature region (up to 400°C).

Another conclusion is that the onset degradation temperatures ($T_{5\%}$) of EP5 to EP20 have an obvious decrease compared to

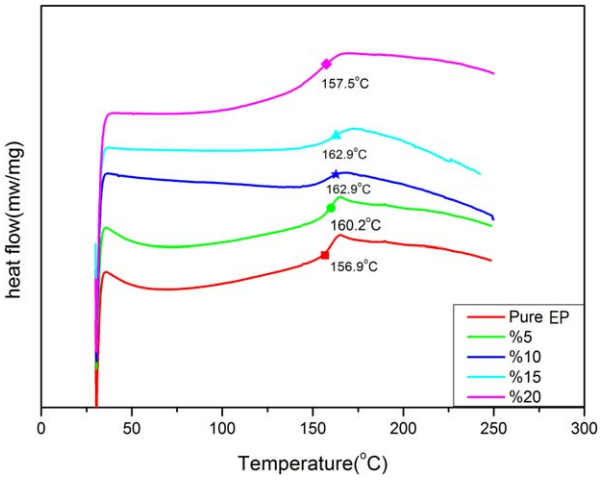

Figure 7. DSC curves of pure EP and modified EP with different DOPO–TVS contents. [Color figure can be viewed in the online issue, which is available at wileyonlinelibrary.com.]

that of the pure EP. This can be attributed to the degradation of the hybrid phosphorus-containing flame retardant in relatively low temperature region.

As to the DTG curves [Figure 6(b)], the most distinguished phenomenon is that the maximum heat loss rate of the silicon/phosphorus-containing EP is much lower than that of the pure EP. The result shows a perfect inverse relationship between the DOPO–TVS content and the maximum weight losing rate .The maximum weight losing rate of the pure EP I s 2.14%/°C at 404°C, while that of the hybrid material with 20% DOPO–TVS is only 0.85%/°C at 387.6°C which is less than 40% of that of the pure EP. This can be explained that the phosphorus-containing groups decompose at low temperature and then generate phosphorus-rich char yield which covers on the surface of the specimen to inhabit decomposition. Meanwhile, the Si—O—Si bonds break and aggregate in the char yield, enhancing the thermal stability of the char yield significantly. However, T_{max} of the modified resins slightly decreases compared to that of pure EP. This can also be attributed to the prior decomposition of the phosphorous bonds. The data of thermal stability is shown in Table II in detail.

Flame resistance can be quantified from the LOI test. Van Krevelen established a linear relationship between LOI and char

Table II. Thermal Stability and Flame Retardancy of the Samples

Sample	$T_{5\%}$ (°C)[a]	T_{max} (°C)[b]	$(dM/dT)_{max}$ (%/°C)[c]	Char yield (%)[d]	T_g (°C)	LOI (%)
EP	385.2	404	−2.14	21.7	156.9	22.5
EP5	350.5	400.5	−0.99	29.5	160.2	26.0
EP10	341.5	401.5.	−0.95	31.7	162.9	32.0
EP15	347.6	387.6	−0.86	28.4	162.9	30.2
EP20	348.4	380.9	−0.85	28.2	157.5	28.5

[a] $T_{5\%}$, the temperature when 5% weight loss occurs.
[b] T_{max}, the maximum weight losing temperature.
[c] $(dM/dT)_{max}$, the maximum weight losing rate.
[d] Char yield at 600°C.

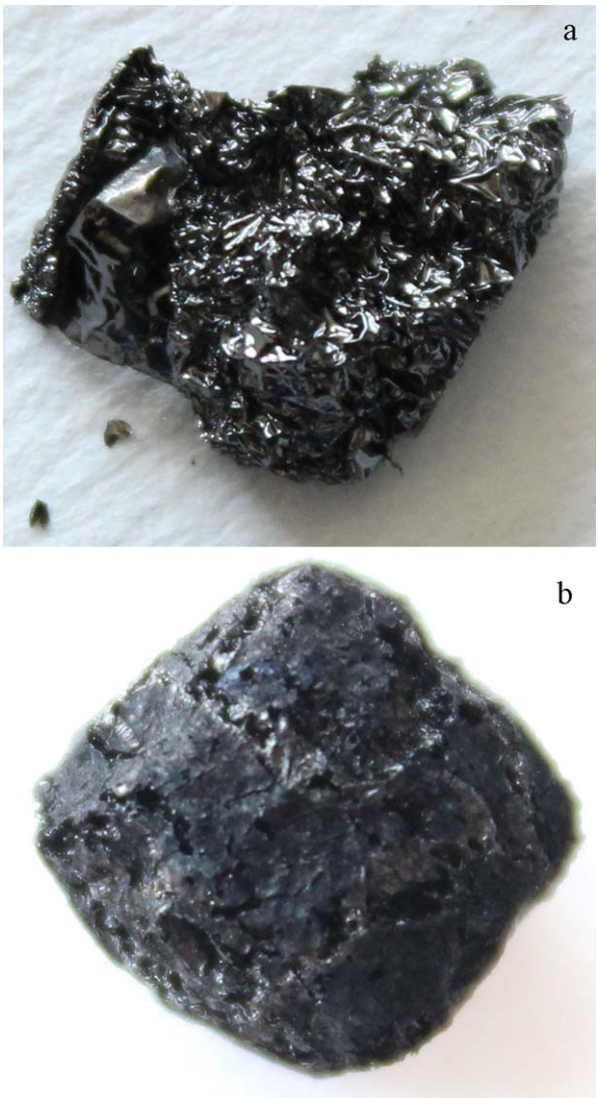

Figure 8. Photographs of char residue of pure EP (a) and EP10 (b). [Color figure can be viewed in the online issue, which is available at wileyonlinelibrary.com.]

residue for halogen-free polymers.[24] The generation of combustible carbon-containing gases is limited, and the exothermicity decreases along with the increasing of char yield thus a higher char yield will enhance flame retardancy. LOI of the EP10 exhibits the highest LOI value of 32 which is consistent with the result of the char yield.

DSC was carried out to investigate glass transition temperature of the modified EP (Figure 7). It is reported that the introduction of Si—O—Si bond can obviously increase the T_g of the EP due to its high bond energy.[25–28] However, there is only a slight increase of T_g for the final cured EP. It may be concluded that the big Si—O—Si groups results in bulk pendants in the basic epoxy network and hindered the crosslinking of EP. The bulk pendants may expand the grid gap thus increase the free volume and reduce the crosslink density of the cured resin. The raised T_g for EP5 to EP20 may be caused by that the positive effect of high bond energy of the Si—O═Si structure on T_g has advantages over its influence of decreased crosslinked density which will lower T_g.[28] The result of DSC is consistent with other thermal analysis that EP10 exhibits the best thermal stability because of the good organic–inorganic network due to proper content of DOPO–TVS.

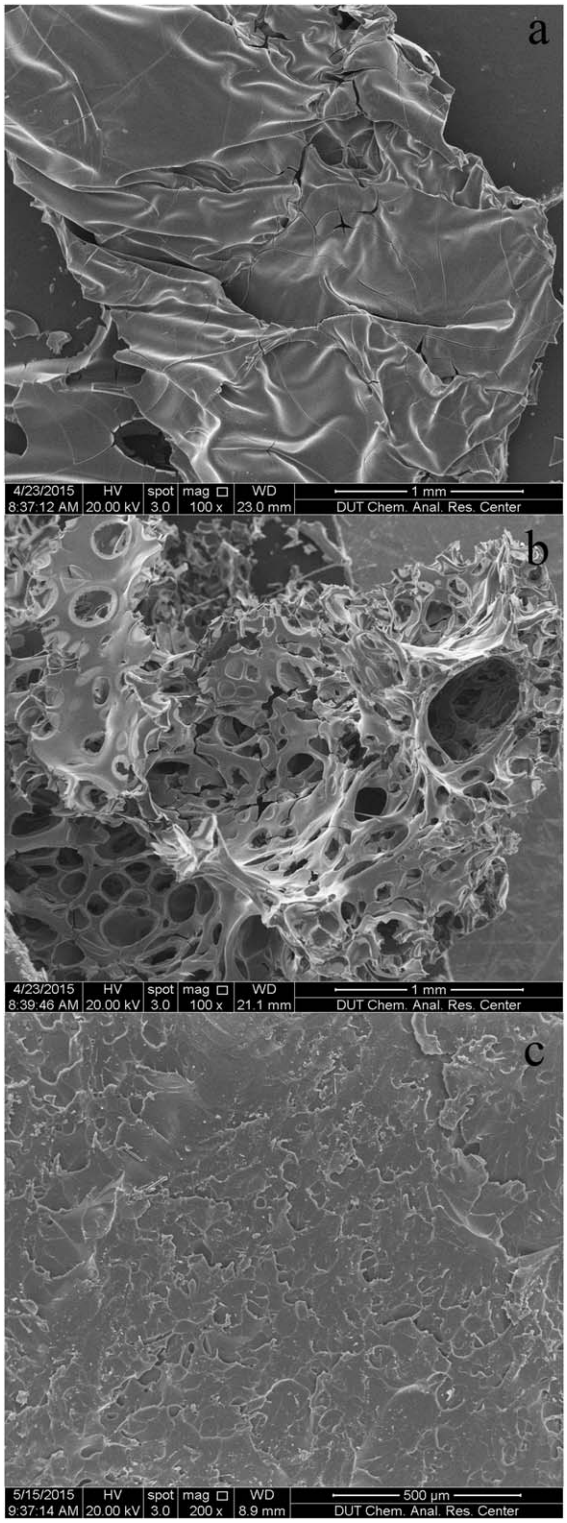

Figure 9. SEM images of char layers (a: pure EP; b: inner char layer of EP10; c: exterior char layer of EP10).

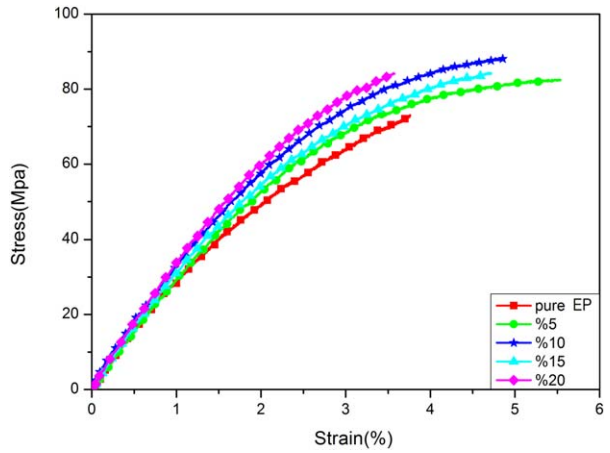

Figure 10. Stress/stain curves. [Color figure can be viewed in the online issue, which is available at wileyonlinelibrary.com.]

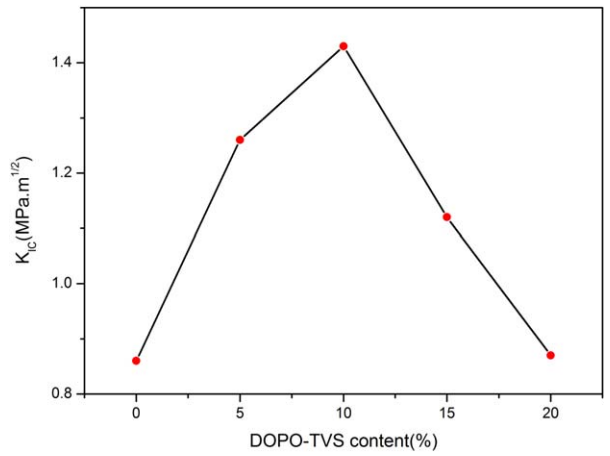

Figure 11. The broken line of K_{IC}. [Color figure can be viewed in the online issue, which is available at wileyonlinelibrary.com.]

Visual Observation

The cured EP was heated to 650°C at a rate of 5°C/min in a tube furnace to obtain the char residues after thermal degradation in air atmosphere. Unfortunately, for the pure EP, almost no residue could be detected under this temperature. To get visible char residue, the final heating temperature was lowered to 550°C. The char residue for pure EP displays an obviously intumescent appearance which barely remained a thin surface layer even though under a relatively low temperature [Figure 8(a)]. The surface layer is glossy and compact which shows that the resin matrix melted and condensed after cooling down. As a distinct comparison, the char residue of silicon/phosphorus containing EP remained their original profile with a highly crosslinked char layer [Figure 8(b)]. This dense char layer held the original shape of the specimen, cut off the O_2 supply, and thus restricted the decomposition and combustion.

SEM Analysis

Figure 9(a) shows the SEM of the char residue of pure EP after heating to 550°C. The residue is glossy with obvious ripple and fold which confirms that the matrix melted during heating process and condensed after cooling down. We can see that the chars of Si/P containing resin exhibits a crosslinked structure with intensive microholes in the SEM image of inner structure [Figure 9(b)]. These microholes should be attributed to the migration of silicon and phosphorus to the surface. This explanation is confirmed by the morphology of the surface. Compact charred layers are observed on the outer surface of the residues [Figure 9(c)] which effectively protect the internal structures and inhibit the heat transmission and isolate the inner material from O_2 outside.

Mechanical Behavior

Figure 10 shows the stress/strain curves of the pure EP and modified EPs with different amounts of DOPO–TVS. Improved tensile strength and failure strain of the modified EPs are detected simultaneously, only EP20 exhibits slightly depressed failure strain compared to the pure EP. The introduction of

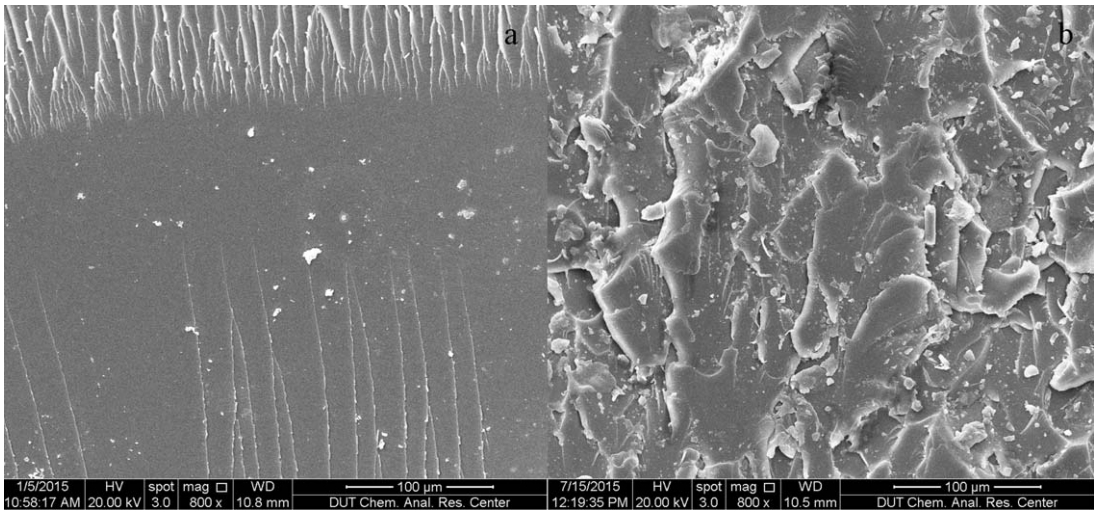

Figure 12. SEM images of cross-section in ×800 magnification after tensile test (a) pure EP (b) EP10.

Table III. Mechanical Properties of the Samples

Sample	Stress (MPa)	Strain (%)	K_{IC} (MPa $m^{1/2}$)
Pure EP	73	3.76	0.86
EP5	82.36	5.54	1.26
EP10	87.99	4.86	1.43
EP15	84.29	4.72	1.12
EP20	84.13	3.58	0.87

DOPO–TVS possessing the Si—O—Si structure could remarkably enhance the tensile properties of the EP. Figure 11 demonstrates the broken line of fracture toughness (K_{IC}) of the EPs as a function of the DOPO–TVS loading. K_{IC} of the modified resin significantly increases until the DOPO–TVS loading reaches to 10%. To present an evidence of the improved mechanical properties, SEM was used again to observe the tensile fracture section of specimen pure EP and EP10 which are shown in Figure 12(a,b). Clear river lines and smooth area were observed for the pure EP, as shown in Figure 12(a), which is a typical brittle feature. As shown in Figure 12(b), for EP10, the fracture surface is accompanied with a large amount of ductile sunken areas, indicating a typical tough feature. It suggests that the incorporation of DOPO–TVS effectively resists crack propagation and increases the strength and toughness.[29,30] When the DOPO–TVS loading is 15%, obvious deterioration of K_{IC} emerges compared to EP10. As the DOPO–TVS loading further raises to 20%, K_{IC} of the modified EP continues to decrease, almost being equal to that of the pure EP. The test data of mechanical properties are listed in Table III in detail. The tensile stress and K_{IC} of EP10 increase by 20% and 66%, respectively. These phenomena reveal that the self-condensation of excess siloxane monomers induced by the high DOPO–TVS content generates big bulk pendants which results in microdefect in the matrix thus influences the toughness of the composite

CONCLUSIONS

A phosphorus–silicon containing flame retardant was prepared with DOPO and TVS. Then hybrid phosphorus–silicon containing EP was synthesized. Phosphorus and silicon were introduced into the matrix in the form of silica network via conventional sol–gel process. The resulted modified resin was characterized through FTIR and NMR. Improved thermal stability and flame retardancy were confirmed through TGA and LOI test. The maximum weight losing rate for the modified EP notably declined and the charring yield increases as high as 46% compared to the pure EP. Char residue was observed through SEM .Compact surface layer and poriferous inner morphology were confirmed which demonstrated the synergy effect of phosphorus and silicon on flame retardancy. Tensile test and fracture toughness were carried out to explore the influence of the modification on the EP. The tensile stress and K_{IC} of EP10 increase by 20% and 66%, respectively, compared with that of pure EP. SEM was used again to reveal the fracture morphology after tensile test. The cross-section of modified EP shows a typical tough feature. The results show a noticeable mechanical strengthening potential of the silica network when proper content of DOPO–TVS be incorporated into the EP. In summary, the introduction of the flame retardant DOPO–TVS can improve the thermal stability and flame retardancy as well as the mechanical properties.

ACKNOWLEDGMENTS

This work was supported by Fundamental Research Funds for the Central Universities (DUT10ZDG05) and the National Natural Science Foundation of China (51102031, 51002019 and 91016024).

REFERENCES

1. Song, J.; Chen, G.; Wu, G.; Cai, C.; Liu, P.; Li, Q. *Polym. Adv. Technol.* **2011**, *22*, 2069.
2. Qian, R.; Yu, J.; Xie, L.; Li, Y.; Jiang, P. *Polym. Adv. Technol.* **2013**, *24*, 348.
3. He, Y.; Chen, C.; Zhong, F.; Chen, H.; Qing, D. *Polym. Adv. Technol.* **2015**, *26*, 414.
4. Zhang, W.; Li, X.; Yang, R. *Polym. Adv. Technol.* **2013**, *24*, 951.
5. Zang, L.; Wagner, S.; Ciesielski, M.; Müller, P.; Döring, M. *Polym. Adv. Technol.* **2011**, *22*, 1182.
6. Iji, M.; Kiuchi, Y.; Soyama, M. *Polym. Adv. Technol.* **2003**, *14*, 638.
7. Wang, X.; Hu, Y.; Song, L.; Xing, W.; Lu, H. *Polym. Adv. Technol.* **2012**, *23*, 190.
8. Bai, Z.; Jiang, S.; Tang, G.; Hu, Y.; Song, L.; Yuen, R. K. K. *Polym. Adv. Technol.* **2014**, *25*, 223.
9. Gérard, C.; Fontaine, G.; Bourbigot, S. *Polym. Adv. Technol.* **2011**, *22*, 1085.
10. Wang, M.; Du, J.; Deng, Q.; Tian, Z.; Zhu, J. *Mater. Sci. Eng. A* **2015**, *626*, 382.
11. Liu, W.; Wang, Z.; Chen, Z.; Li, J. *Polym. Adv. Technol.* **2012**, *23*, 367.
12. Farah, S.; Aviv, O.; Laout, N.; Ratner, S.; Beyth, N.; Domb, A. J. *Polym. Adv. Technol.* **2014**, *25*, 689.
13. Zhao, M.; Feng, Y.; Li, G.; Li, Y.; Wang, Y.; Han, Y. *Polym. Adv. Technol.* **2014**, *25*, 927.
14. Sun, B.; Qin, D.; Liang, G.; Gu, A.; Yuan, L. *Polym. Adv. Technol.* **2013**, *24*, 1051.
15. Gao, S.; Li, B.; Bai, P.; Zhang, S. *Polym. Adv. Technol.* **2011**, *22*, 2609.
16. Burunkaya, E.; Kesmez, Ö.; Kiraz, N.; Çamurlu, H. E.; Asiltürk, M. *Thin Solid Films* **2012**, *522*, 238.
17. Peng, S.; Zeng, Z.; Zhao, W.; Li, H.; Xue, Q.; Wu, X. *Surf. Coat. Technol.* **2012**, *213*, 175.
18. Papkov, M. S.; Langer, R.; Domb, A. J. *Polym. Adv. Technol.* **2011**, *22*, 502.
19. Chernyy, S.; Ulah, S.; Sørensen, G.; Tordrup, S. W.; Pedersen, P. B.; Almdal, K. *J. Appl. Polym. Sci.* **2015**, *132*, 41955.
20. Farah, S.; Khan, W.; Farber, I.; Shvero, D. K.; Beyth, N.; Weiss, E. I.; Domb, A. *J. Polym. Adv. Technol.* **2013**, *24*, 446.

21. Nazir, T.; Afzal, A.; Siddiqi, H. M.; Ahmad, Z.; Dumon, M. *Prog. Org. Coat.* **2010**, *69*, 100.
22. Chiang, C. L.; Ma, C. C. *Eur. Polym. J.* **2002**, *38*, 2219.
23. Chiang, C.; Chang, R.; Chiu, Y. *Thermochim. Acta* **2007**, *453*, 97.
24. Krevelen, D. W. *Polymer* **1975**, *16*, 615.
25. Ickowicz, D. E.; Zada, M.; Abbas, R.; Touitou, D.; Nyska, A.; Golovanevski, L.; Weiniger, C. F.; Katzhendle, J.; Domb, A. J. *Polym. Adv. Technol.* **2014**, *25*, 1323.
26. Chiang, C.; Chang, R. *Compos. Sci. Technol.* **2008**, *68*, 2849.
27. Ponyrko, S.; Kobera, L.; Brus, J.; Matějka, L. *Polymer* **2013**, *54*, 6271.
28. Kuan, C.; Chen, W.; Li, Y.; Chen, C.; Kuan, H.; Chiang, C. *J. Phys. Chem. Solids* **2010**, *71*, 539.
29. Peng, D.; Qin, W.; Wu, X. H. *Acta Astronaut.* **2015**, *111*, 84.
30. Qi, B.; Lu, S. R.; Xiao, X. E.; Pan, L. L.; Tan, F. Z.; Yu, J. H. *Expr. Polym. Lett.* **2014**, *8*, 467.